No. 128/23, 93–107
ISSN 2657-6988 (online)
ISSN 2657-5841 (printed)
DOI: 10.26408/128.06

Submitted: 05.07.2023
Accepted: 18.10.2023
Published: 29.12.2023

ANALYSIS OF ENERGY FLOWS OF A SECTOR-COUPLED POWER GENERATION UNIT (HYDROGEN MICROGRID)

David Stephan[1]*, Uwe Werner[2]

[1,2] Bremerhaven University of Applied Science, Institute for Automation and Electrical Engineering (IAE), An der Karlstadt 8, 27568 Bremerhaven, Germany,

[1] e-mail: dstephan@hs-bremerhaven.de

*Corresponding author

Abstract: This paper investigates the dynamic characteristics of the energy flows of the energy sectors electricity, heat, and gas, and evaluates the necessary components of the reconversion chain during operation. In addition to providing electrical energy, the H_2 microgrid can also serve as a heat and gas supplier by generating the gas (hydrogen) within the electrolysis plant, storing it at different pressure levels, and then making it available to other processes. Furthermore, the electrical energy sector is addressed, where batteries, power electronics, electrical loads of the microgrid are analysed for their behaviour and impact on grid stability. Finally, the overall efficiencies of the coupling between the electric power and gas sectors resulting from the electrolyser and the fuel cell are compared and evaluated.

Keywords: hydrogen, microgrid, power-to-gas, sector-coupled, power generation unit.

1. INTRODUCTION

The interaction of generation, distribution, and storage of electrical energy as part of a sector-coupled energy unit will play an essential role in reducing greenhouse gas emissions CO_2 in the future. It is becoming apparent that there will be a shift from centralised control of the power grid to a decentralised topology of generation and distribution systems with intelligent, self-sufficient supply units. With an increasing share of renewable, decentralised electrical generation units such as photovoltaic or wind power plants, location-based microgrids can make an important contribution to grid-serving supply stability in the energy mix. The microgrid can also provide local reactive power for voltage stability. Surplus electricity from renewable energy sources can thus be regulated more variably and efficiently at the smallest site-specific level.

The microgrid in Figure 1 can also be used as a self-sufficient system for regional neighbourhood supply or as an off-grid application. In addition to providing electrical energy, a microgrid can also serve as a heat and gas supplier by generating

hydrogen within the energy generation unit, storing it, and feeding it back into the grid. The waste heat generated during the processes of sector coupling can then be decoupled and used for further applications. The microgrid shown in Figure 1 was developed at the Bremerhaven University of Applied Sciences and has subsequently been successfully put into operation.

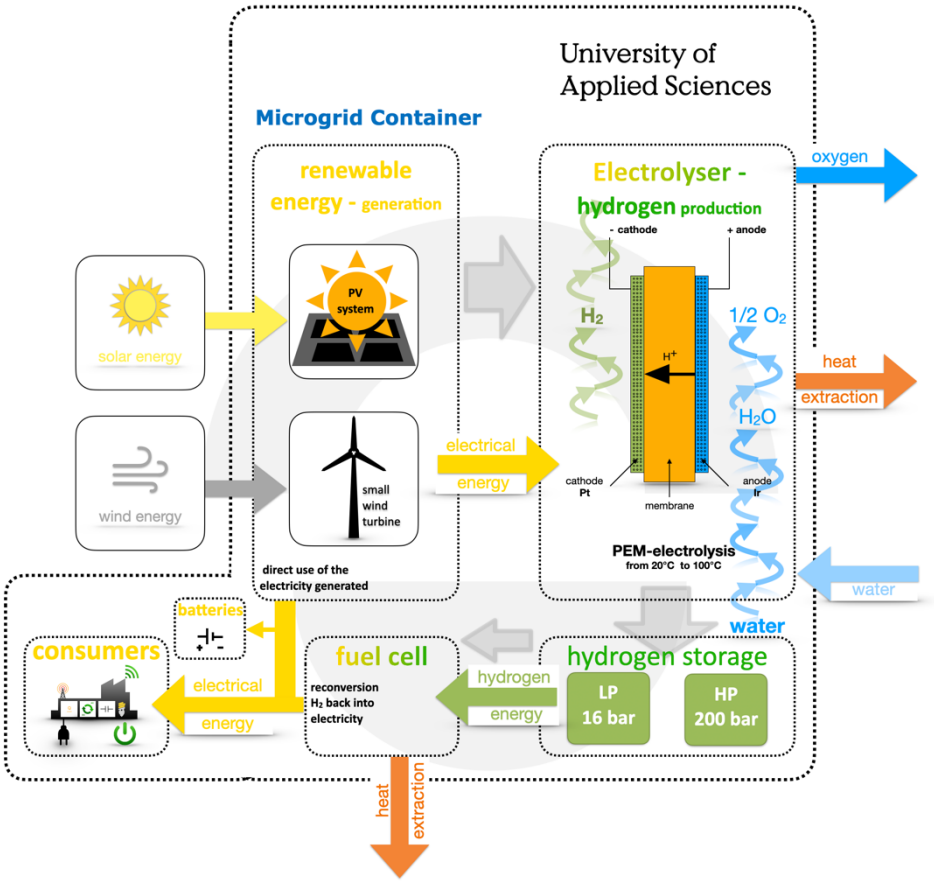

Fig. 1. Energy flow diagram of the sector-coupled energy generation unit (hydrogen microgrid)

The heat extraction in the sector coupling makesthe microgrid system significantly more efficient overall. In the context of this article, the microgrid represents a sector-coupled energy production unit that links the hydrogen, heat, and electrical energy sectors in terms of control technology. This publication is based on the results of the EFRE-funded project "Hydrogen: Green Gas for Bremerhaven",

which were obtained by measurements on the self-constructed microgrid. This paper is intended to evaluate the dynamic energy flows during operation, especially in the electrical sector, since this is where the highest dynamic load requirements are to be expected in transient processes. Among other things, the reaction times of the interconnected energy sectors and their feedback are to be investigated.

2. UTILISATION OF RENEWABLE ENERGY GENERATION

In addition to solar energy, wind energy is also used for the emission-free generation of electrical energy for the self-sufficient energy system. Wind turbines in the MW range are particularly economical, as it is possible to achieve attractive annual full load hours from the corresponding turbine heights. In the case of the microgrid under investigation, the technically less mature small wind turbines (TRL 7-8) are used as an example for the generation profiles of wind turbines [Hirsch, Parag and Guerrero 2018]. With the additional installation of a photovoltaic system (TRL 9), the goal is to use a maximum share of the generated energy directly, and also in this case there is the possibility to use real generation profiles of PV systems for the simulation.

Individually, the generation profiles for wind and solar energy are subject to strong fluctuations [Olulope, Odetoye and Olanrewaju 2022]. Consequently, an increased expansion of one technology, for example photovoltaics, leads to an increased peak output, but the additional energy can only be used directly to a marginal extent, since the same generation periods are available in which energy is already being generated [Rubenis and Adrian 2018]. Due to the low probability of parallel availability of solar and wind energy, the situation is different. If the same capacity of wind turbines is added, the direct consumption of the system can be increased and, conversely, the storage requirement can be reduced [Hirsch, Parag and Guerrero 2018; Olulope, Odetoye and Olanrewaju 2022].

3. SECTOR COUPLING

The generation, storage and reconversion of hydrogen in the form of the electrolyser, the H_2 low-pressure and H_2 high-pressure storage, the hydrogen compressor and the fuel cell are considered integrally within the gas sector (hydrogen network) *(*Fig. 2).

In the heat sector, the waste heat generated by the electrolyser and fuel cell is investigated together with the central recooler for heat extraction. Furthermore, the electrical energy sector is examined by analysing the behaviour of batteries, power electronics and electrical consumers of the microgrid and their influence on grid stability.

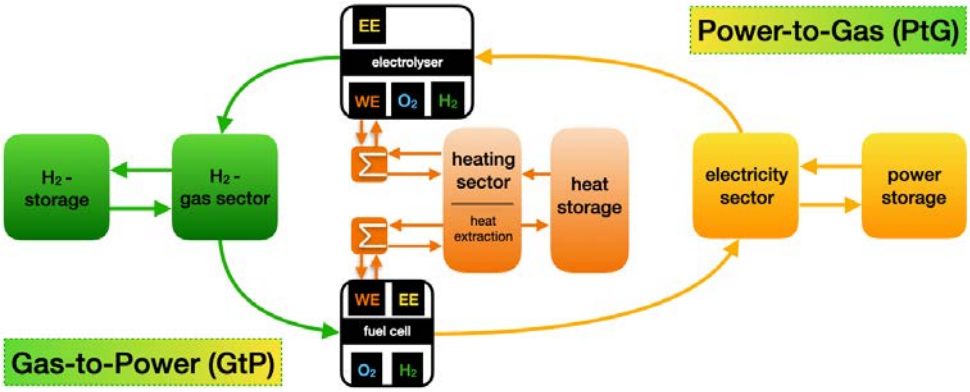

Fig. 2. Sector coupling of the energy generation unit power-to-gas (electrolyser) and gas-to-power (fuel cell)

3.1. Power-to-Gas (elektrolyser)

The electrolyser can be given different power levels, from which statements can be made about the start-up and control behaviour (dynamics/overshoot) as well as the resulting effects on grid stability.

Figure 3 shows that the values calculated in static operation correspond very well with the measured values. Only after the electrolyser is switched off are the values significantly higher (cf. Figure 3). This dynamic deviation results from the physical measuring principle (variable area flow sensor) and has little or no effect on the operation.

Consequently, as an alternative to determining the efficiency of the electrolyser, the filling level of the low-pressure storage tank or its increase or decrease is used as the basis for determining the exact amount of hydrogen generated. The pressure change from static to dynamic pressure can be shown on the basis of the pressure curve of the H_2 low-pressure storage tank (cf. Fig. 3). The slope of the curve can be used to draw conclusions directly about the hydrogen storage and also about the power consumption of the electrolyser. The steeper the pressure rise in the low-pressure storage tank, the higher the hydrogen production and the associated hydrogen volume produced by the electrolyser.

In the evaluated measurement period, a water consumption of 2 l was determined in relation to the generation of 0.2 to 0.25 Nm^3 H_2. This results in a water consumption eight to nine times higher than chemically necessary for hydrogen generation, which is derived from an electrolyser-internal water quality specification of the deionisation system (reverse osmosis). While this is not a problem for operating sites with sufficient water supply, it must be considered more closely in

the context of increasing water scarcity and a general conservation of resources in subsequent projects.

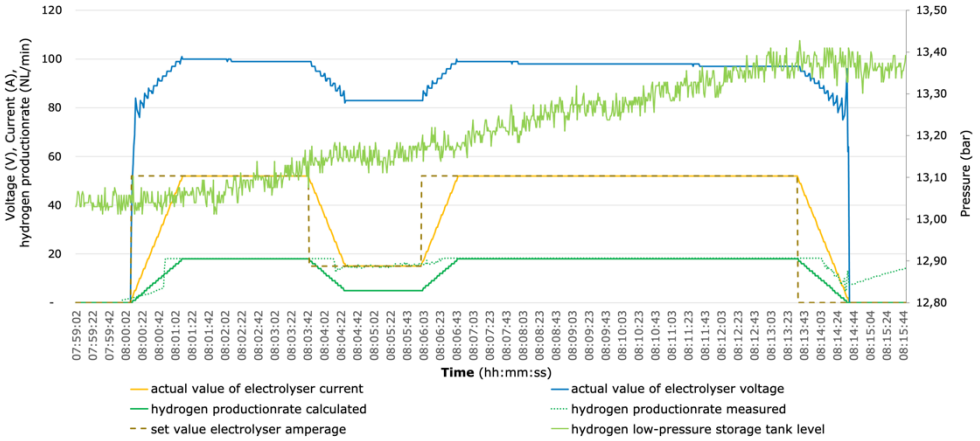

Fig. 3. Reaction performance and generation analysis of an electrolyser in the field

3.2. Gas-to-power (fuel cell)

The fuel cell is given load levels in the form of current and voltage setpoints, which have an effect on start-up and control behaviour and ultimately on grid stability. In addition, the jumps in the absorbed voltage, due to the chemical process of the fuel cell, have an influence on the dynamics (reaction time). The voltage jump results from the fact that sufficient voltage must first be built up within the cells before air and hydrogen can react to form water (cf. Fig. 4). The fuel cell is thus an inductive generator during start-up and a capacitive generator during run-down.

In Figure 4, the curves of the voltage and current of the fuel cell are compared with the filling level (filling pressure) of the low-pressure water storage tank. The pressure fluctuations caused by the opening and closing of the gas valve, which serves to protect the fuel cell against excessive pressure surges and venting, are striking. This valve is installed between the fuel cell and the hydrogen tank. The pressure curve of the low pressure hydrogen storage tank shows the pressure change from static to dynamic pressure (Fig. 4). The slope of the curve can be used to draw direct conclusions about the hydrogen consumption and thus the performance of the fuel cell. The steeper the pressure drop in the low-pressure storage tank, the higher the hydrogen consumption and the associated electrical power generated by the fuel cell. When the operating state of the fuel cell changes from "standby" to "operating" mode, the voltage is first ramped up and maintained and then the current is ramped up in a controlled manner.

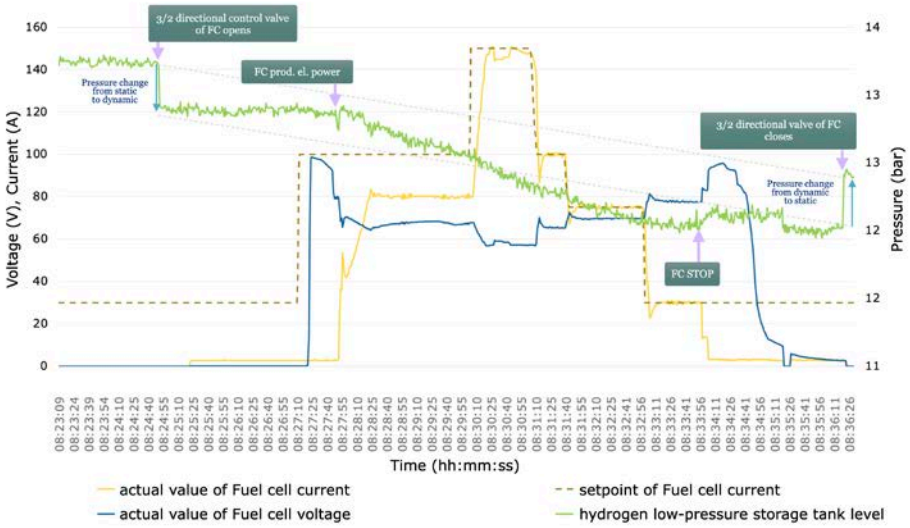

Fig. 4. Consumption analysis and driving behaviour (dynamics) of a fuel cell in the field

This leads to a serious loss of dynamics, which rules out the use of a fuel cell alone for highly dynamic applications. This is the main reason why a battery cannot be dispensed with in fuel cell systems, as it serves as a buffer storage (dynamic current output) to cover the high dynamic requirements for load transients. In this case, however, the size of the battery storage is only a fraction of what a pure battery storage must have for the comparable power and storage size.

The electrical power output of the fuel cell increases with increasing current. When looking at the setpoint and actual curves of the current curves, high control deviations occur during start-up, which can be attributed to the "cold start" of the fuel cell.

This means that the current can only be further increased when a certain operating temperature is reached. On the other hand, typical overshoots, such as occur with PI control, are evident when the power product within the fuel cell is shut down. These always occur when the setpoint is changed. Subsequently, the actual value of the fuel cell amperage settles to the setpoint value and there is an acceptable control deviation.

In the heat sector, when the waste heat of the fuel cell is used, similar significant control losses occur. Figure 5 shows the flow and return temperature curves of a fuel cell (FC). At the beginning, the input temperature value of the cooling circuit is within the recommended temperature range of 20 °C to 30 °C. The fuel cell is then cooled down to the recommended temperature. Over the entire measurement period, the fuel cell was operated at an average of 30 % of its maximum production output. In the process, the cooling temperature of the fuel cell increases by 11 K/min.

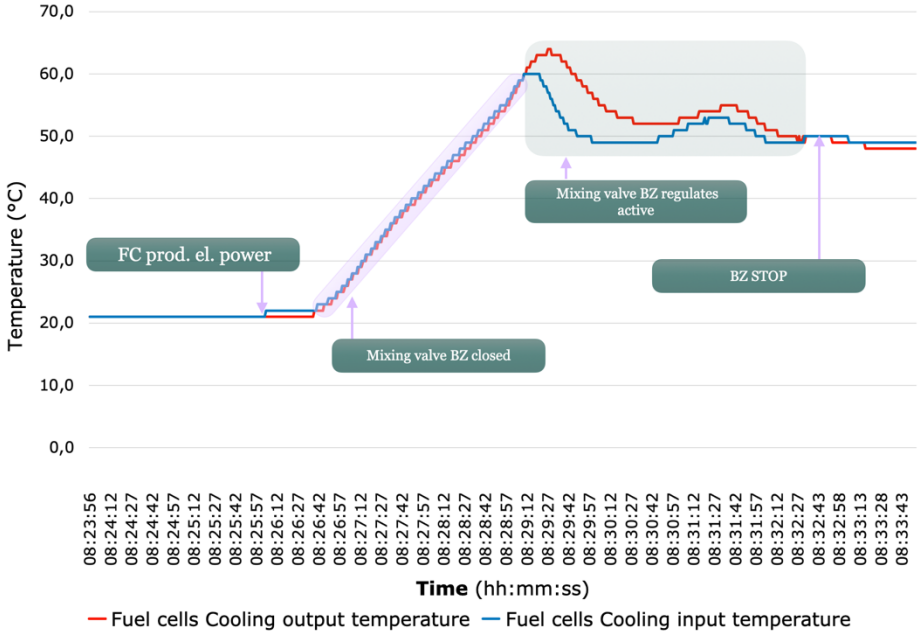

Fig. 5. Cooling circuit of the fuel cell including inlet and outlet temperature curves

Since the temperature rise of flow/return is the same at the beginning of the power output, this is a control with a mixing valve. The latter is initially closed and is actively controlled when the set operating temperature is reached and a delta T between 4 and 6 Kelvin is set. When the fuel cell is switched off, the mixing valve is closed, and the inlet and outlet temperatures approach each other again. This heat span of 6 K and the temperature level of approx. 60 °C can be used for standard heating applications in building structures.

4. ENERGY STORAGE SYSTEMS

The energy storage systems of the microgrid shown in Figure 6 consist of electrical, electrochemical, and chemical storage forms. These three forms of energy storage are necessary due to various fluctuation patterns in the feed-in of electrical energy from wind and sun, as they can provide electrical energy for different periods of time. Here, the reaction time, the dynamic course of the energy output and the maximum storage capacity play a role in evaluating the usability as an energy supply system in the electrical grid.

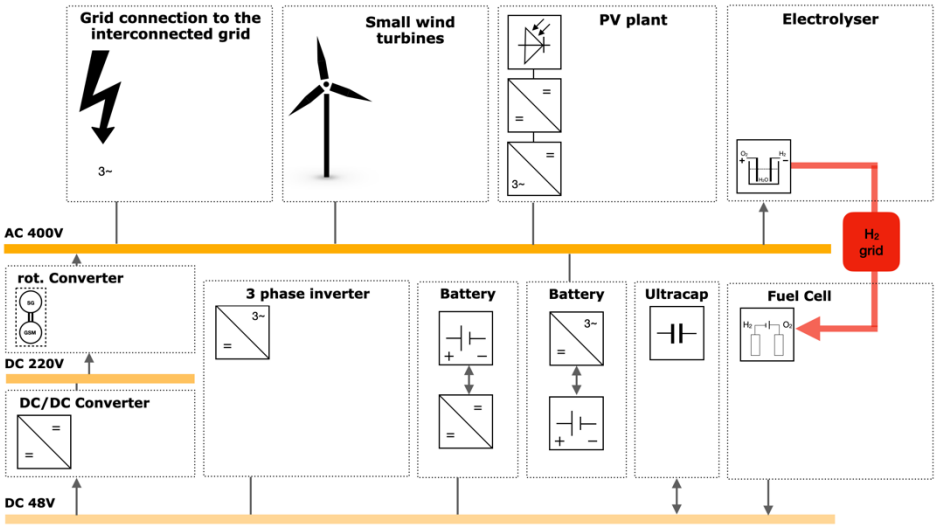

Fig. 6. Electrical grid structure of the microgrid

Battery storage systems represent the electrochemical form of energy storage. They are used for secondary control, act as an hourly reserve and have an influence on the reactive power of the system. They represent the short-term storage within the microgrid.

The battery storage comprises a maximum of 15% of the entire energy storage system of the microgrid. With the stored electrical energy, a two-person household with a total consumption of 2500 kWh/a could be supplied self-sufficiently for four days.

The chemical form of energy storage is represented by the hydrogen storage system and is used for the seasonal balancing of fluctuating renewable energy generation. The hydrogen storage takes up 85% of the energy storage. By converting the hydrogen back into electricity with the help of the fuel cell, a 2-person household can be supplied self-sufficiently with 2500 kWh/a for 21 days. Unlike a battery storage system, the hydrogen storage system is independent in its design of "charging and discharging power". It is possible to combine different electrical power classes for an electrolyser and fuel cell. As a result, smaller electrolysers can be used for peak shaving during the energy-rich months of renewable energies. However, it is also possible to provide the entire electrical power from the storage system with a larger fuel cell on days, weeks or months when hardly any renewable energy from wind and sun is available.

Figure 7 shows the temperature-dependent pressure fluctuations in the low- and high-pressure storage system for 24 hours.

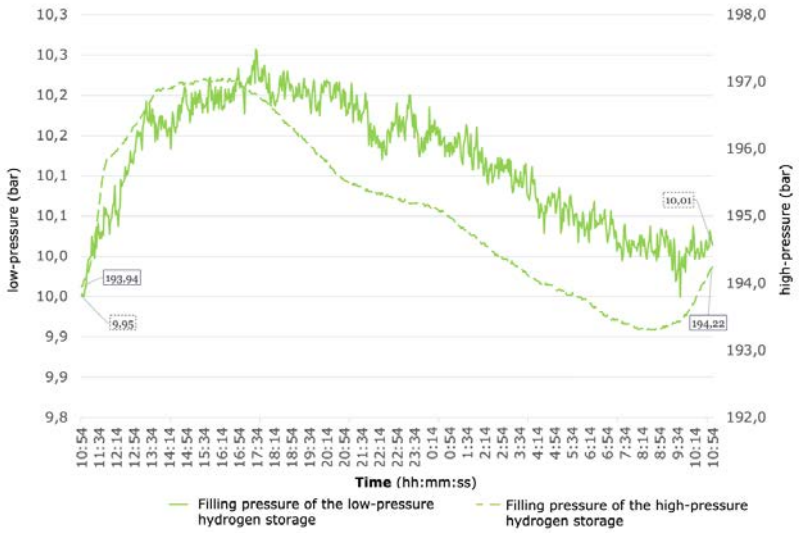

Fig. 7. Temperature-dependent pressure fluctuations of the hydrogen storage system – Long-term storage

The temperature curve in Figure 8 (cf. Fig. 7) confirms the linear dependence on a closed gas system. Accordingly, the changes can be interpreted as a direct result of the fluctuating temperature during the day. Overall, no significant losses can be detected in the hydrogen storage system, even over a longer measurement period.

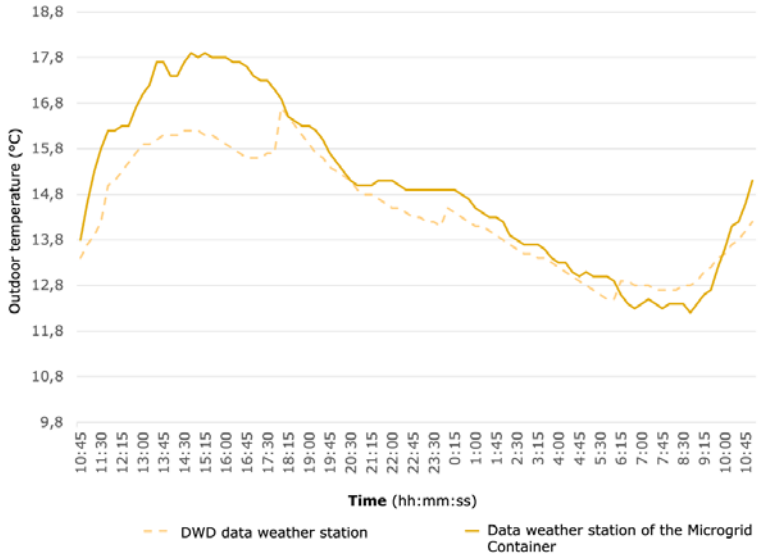

Fig. 8. Comparison of the measured temperatures and the DWD for Bremerhaven

The third type of storage for electrical energy is described by the built-in supercapacitor with 165 Farad and a peak current of 2000 A. This is used to compensate for high start-up currents of electrical consumers in the millisecond range [Stephan, Werner and Fichter 2022a,b].

5. HEAT EXTRACTION

In Figure 9, the heat sector is represented by the waste heat generated during operation by the electrolyser and fuel cell in connection with the central re-cooler for heat extraction. The total cooling circuit consists of a central primary and 2 decentralised secondary cooling circuits. Starting with the secondary circuit of the electrolyser, which must serve a heat output of up to 2 kW. At a maximum electrical power consumption at the beginning of the electrolyser's lifetime, this suggests a hydrogen production rate of 1 Nm3/h. The inlet temperature of the electrolyser should be in the range of 20 °C to 30 °C at the beginning of operation. During operation, an initial temperature of approx. 60 °C and a delta T of 6 °C to 8 °C is reached.

The second secondary circuit of the sector-coupled energy generation unit is determined by the characteristics of the fuel cell. This produces a waste heat of 9.9 kW with a maximum electrical power output of 7.8 kW [Proton Motor Fuel Cell GmbH 2018].

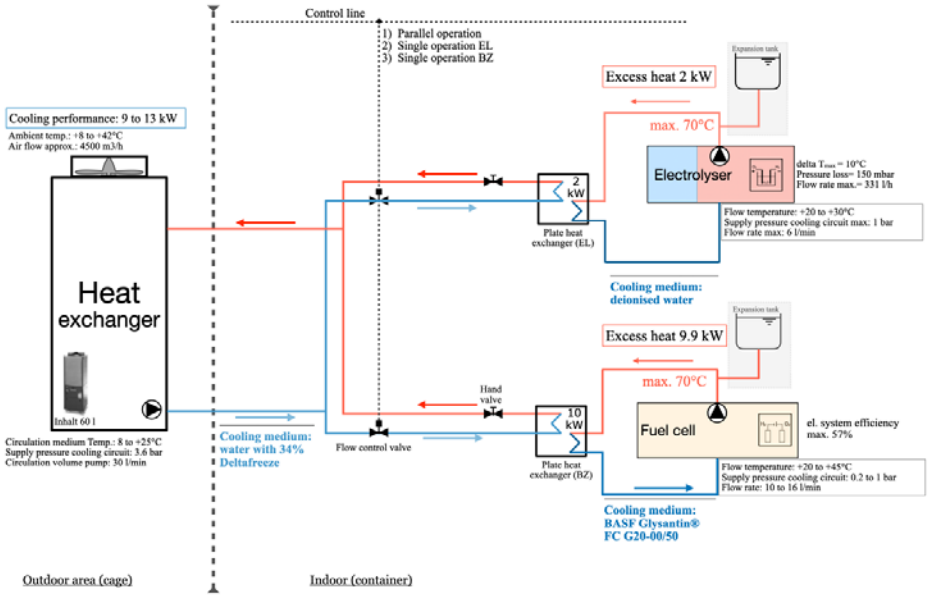

Fig. 9. Heat extraction of the sector-coupled energy generation unit

A detailed description and illustration of the temperature curve and the control of the secondary circuit of the fuel cell can be found in section 3.2 and in Figure 5. The central primary cooling circuit serves on the one hand to cool the two secondary circuits, and on the other hand as an interface for the subsequent heat extraction and central utilisation of the heat generated by sector coupling.

The total heat output of the microgrid thus amounts to approx. 12 kW, in a temperature range of 50 to 60 °C. This temperature range is perfectly suitable as a supply flow, and it is certainly suitable as a flow temperature for surface heating systems, such as underfloor heating systems [Laasch and Laasch 2013]. By using the waste heat, the level of efficiency can be increased by 20 percentage points [Starmühler 2020].

6. MEASUREMENT RESULTS AND EVALUATION

6.1. Electrolyser

The differences at the start and end of measurement (delta) and the linear approximation are used as the basis for determining the efficiency and dynamic behaviour of the electrolyser. This is contrasted with the performance data of the electrolyser, measured at the electrolysis unit (stack), and the current total consumption of the microgrid, measured at the grid connection point (NVP), which includes any peripheral devices that are necessary for the electrolyser to operate.

The pressure fluctuations caused by opening and closing of hydrogen supply between the electrolyser and the hydrogen storage tank are noticeable here.

Figure 10 provides an overview of the efficiencies determined in the test, the manufacturer's data and the data from the literature. With the exception of the peripheral measurement, there is some consistency in that the partial load range is more efficient than the full load range.

This correlation is crucial for the operation of the electrolysis plant for gas production from renewable sources in order to achieve the maximum utilisation rate for the "green electricity".

Since the peripheral devices have an approximately constant consumption, the observed difference in efficiency can be explained by a lower share of the electrolyser in the total consumption compared to full-load operation.

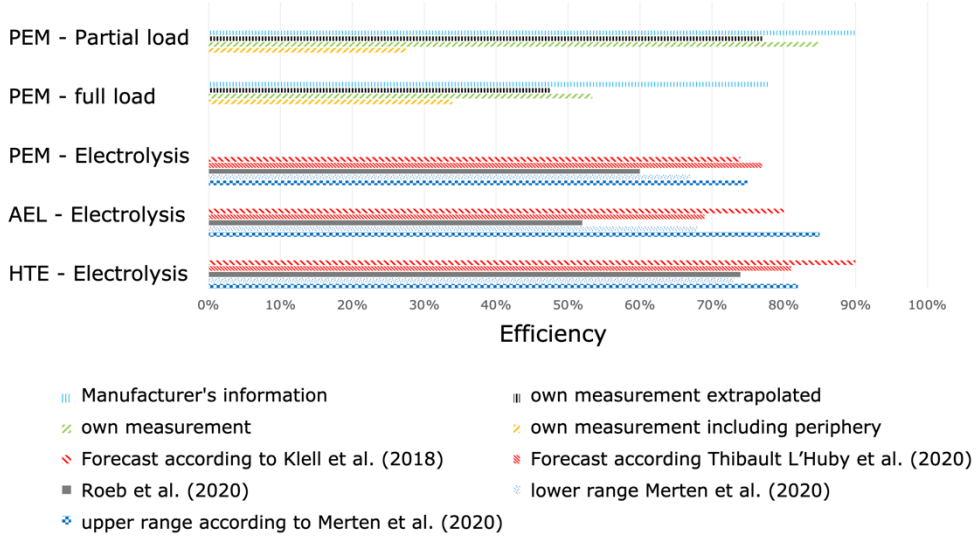

Fig. 10. Comparison between literature values of the efficiency of a PEM electrolysis plant with measurement

Source: [Klell, Eichlseder and Trattner 2018; Merten et al. 2020; Roeb et al. 2020; Thibault L´Huby, Gahlot and Debarre 2020; Stephan et al. 2022].

6.2. Fuel cell

The data basis for determining the fuel cell efficiencies are, on the one hand, the pressure changes of the hydrogen storage tank at the start and end of the measurement (delta) and, on the other hand, the linear approximation (extrapolated). This is contrasted with the performance data of the fuel cell, measured at the stack.

Figure 11 provides an overview of the efficiencies determined in the test in comparison to manufacturer and literature values. Efficiencies in comparison to manufacturer and literature values. Particularly in the partial load range, the manufacturer's specifications correspond to the measurement results.

In full-load operation, the determined efficiencies are only slightly higher than the manufacturer's specifications and correspond to general information from the literature.

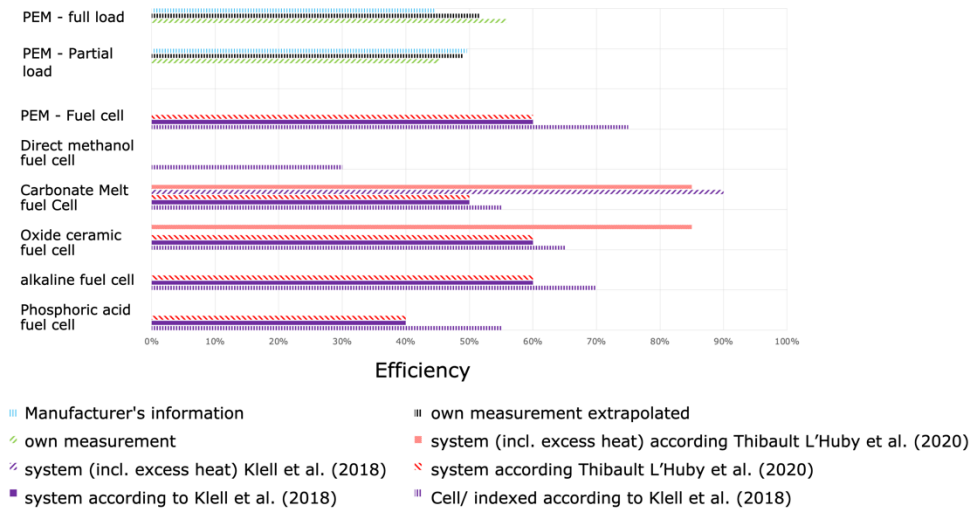

Fig. 11. Comparison between literature values of the efficiency of a PEM fuel cell with measurement results

Source: [Klell, Eichlseder and Trattner 2018; Thibault L´Huby, Gahlot and Debarre 2020; Stephan et al. 2022].

7. CONCLUSIONS

The design and operation of the sector-coupled power generation unit with the requirements for sufficiently high electrical load dynamics can be considered successful. It can be stated that the system is able to supply itself over a period of several weeks without the need to supply additional renewable energy to the sector-coupled system and that the system can be used either as a self-sufficient generation unit or as a grid-serving control unit. The permissible temperature ranges of the individual components are within the prescribed and tolerable target ranges and there are no critical disturbances or system failures within the microgrid, even in continuous operation. The efficiency in the power-to-gas and gas-to-power chain is 45% purely electrical. If the waste heat is used, realistic overall efficiencies of up to 70% can be achieved in these systems.

REFERENCES

Hirsch, A., Parag, Y., Guerrero, J., 2018, *Microgrids: A Review of Technologies, Key Drivers, and Outstanding Issues*, Renewable and Sustainable Energy Reviews, vol. 90, pp. 402–411.

Klell, M., Eichlseder, H., Trattner, A., 2018, *Wasserstoff in der Fahrzeugtechnik*, Springer Fachmedien Wiesbaden, Wiesbaden, Germany.

Laasch, T., Laasch, E., 2013, *Haustechnik*, Springer Fachmedien Wiesbaden, Wiesbaden, Germany.

Merten, F., Scholz, A., Krüger, Ch., Heck, S., Girard, Y., Mecke, M., Goerge, M., 2020, *Bewertung der Vor- und Nachteile von Wasserstoffimporten im Vergleich zur heimischen Erzeugung*, Abschlussbericht: Studie für den Landesverband Erneuerbare Energien NRW e. V. Wuppertal Institut, DIW Econ, Wuppertal, Germany.

Olulope, P., Odetoye, O., Olanrewaju, M., 2022, *A Review of Emerging Design Concepts in Applied Microgrid Technology*, AIMS Energy, vol. 10, pp. 776–800.

Proton Motor Fuel Cell GmbH, 2018, *Handbook of Fuelcell, Model PM Module S5/S8*.

Rubenis, A., Adrian, L.R., 2018, *Determining Energy Storage Amount for Development of Novel Microgrid Energy Flow Optimization System with Photovoltaic Energy Generation*, Energy Procedia, vol. 147, pp. 428–437.

Stephan, D.S. et al., 2022, *Anwendungsfall „Microgrids-autarke Einheiten"*, Abschlussbericht, Bremerhaven, Germany.

Stephan, D.S., Werner, U., Fichter, C., 2022a, *Electrical and Hydrogen Microgrid – Energy Control of a Self-Sufficient Supply System Based on a Combined Electrical and Hydrogen Distribution Grid*, Industrie 4.0 Management, vol. 28, pp. 28–32.

Stephan, D.S., Werner, U., Fichter, C., 2022b, *Energy Control of a Self-Sufficient Microgrid Based on a Combined Electrical and Hydrogen Distribution*, 17. Symposium Energieinnovation, Graz, Austria.

Internet sources

Agert, C. et al., 2020, *Wasserstoff als ein Fundament der Energiewende Teil 2: Sektorenkopplung und Wasserstoff: Zwei Seiten der gleichen Medaille*, Abschlussbericht, DLR, Institut für Vernetzte Energiesysteme, Oldenburg, Germany, https://elib.dlr.de/139867/ (Accessed: 12 February 2021).

Roeb, M., Brendelberger, S., Rosenstiel, A. Agrafiotis, Ch., Monnerie, N., Budama, V., Jacobs, N., 2020, *Wasserstoff als ein Fundament der Energiewende Teil 1: Technologien und Perspektiven für eine nachhaltige und ökonomische Wasserstoffversorgung*, Abschlussbericht. DLR, Institut für Solarforschung, https://elib.dlr.de/137796/ (Accessed: 12 February 2021).

Starmühler, H., 2020, *Der Elektrolyseur, der Wasserstoff und die Nutzung*, https://www.energie-bau.at/heizen-kuehlen/3335-der-elektrolyseur-der-wasserstoff-und-dessen-nutzung (Accessed: 16 January 2023).

Thibault L´Huby, Gahlot, P., Debarre, R., 2020, *Hydrogen Applications and Business Model – Going Blue and Green?* https://www.kearney.com/documents/17779499/ 18269679/Hydrogen+applications+and+business+models_single_page.pdf/c72700b3-e66a-6338-82bb-46ca8031e86d?t=1594994670000.